

Validation of an externally oil-cooled 1 kW_{el} HT-PEMFC stack operating at various experimental conditions

P. Bujlo, S. Pasupathi, Ø. Ulleberg, J. Scholta, M.V. Nomnqa, A. Rabiou and B.G. Pollet

Abstract

The performance of 1 kW_{el} 48-cell HT-PEMFC at various experimental conditions is presented, particularly at several CO concentrations (up to 1.0%). Polarization curves measured at various anode (1.0-2.5) and cathode (1.6-4.0) stoichiometries; stack operating temperatures (120-160 °C) and gas pressures (up to 0.5 barg) are reported and analysed. The minimum gas stoichiometries of 1.25 and 2.0 were determined for the anode and cathode, respectively. The highest stack power density of 225 mW cm⁻² was measured at 160 °C and 0.4 A cm⁻². Operation at CO concentrations up to 1% was achieved, although a loss of performance of about 4% was observed for low CO concentrations. The operating temperature enhanced fuel cell performance and tolerance to CO, even when supplied with higher CO concentration in the anode feed gas.

1. Introduction

High Temperature Proton Exchange Membrane Fuel Cells (HT-PEMFC) have many advantages in comparison to Low Temperature (LT) PEMFC due to their wide operating temperature range 120-200 °C. The proton conduction mechanism that is dependent on the phosphoric acid content [1,2] and not on the humidification level of the proton exchange membrane [3,4] consequently eliminates the need for the supplied reactants to be humidified. Complex water management systems are therefore not required thus simplifying the system design and minimizing the number of Balance of Plant (BoP) components. Furthermore, larger difference between 'ambient' and fuel cell operating temperature makes it possible to recover the hitherto waste heat leading to improve heat integration. The higher operating temperature also simplifies the stack construction, in which the excess heat can be efficiently removed with a coolant passing externally rather than having an internal cooling manifold complicating the stack design. In literature, research and development work results on internally liquid-cooled [5] and air-cooled [6] HT-PEMFC stacks are reported. The design and benefits of an externally cooled HT-PEMFC stack have been reported elsewhere [7-9]. Most importantly the advantage expected from HT-PEMFC is the high operating temperature making HT-PEMFC more tolerant to impurities present in the reactant gases. Especially important from the application

point of view is the improved resistance to carbon monoxide (CO) poisoning [10,11]. This feature enables a HT-PEMFC stack to be directly fed from reforming products eliminating complex purification systems. LT-PEMFC cannot handle CO levels above 10 ppm [12], requiring the use of a reformer with a CO cleaning system to deliver hydrogen rich gas with almost no CO, making the system complicated and costly.

Although high CO tolerances (up to 5% CO) were reported for HT-PEMFCs using single cell measurements [13,14], the number of reports on the CO tolerance for HT-PEMFC stacks is limited in literature. Nevertheless, there are a few reports, for example Mocoteguy et al. [15,16], that published results of long-term testing of HT-PEMFC stack in dynamic and continuous mode at 1% CO concentration. It is important to study the CO tolerance of the HT-PEMFC stack and thereby prove its expected advantage. The present paper includes the description of a prototype HT-PEMFC stack construction, experimental procedure and results of its validation under various operating conditions. This investigation reports results of experimental work that has been carried out on the performance of a 1 kW HT-PEMFC stack operating under various anode and cathode stoichiometries, stack temperature and pressure as well as wider CO concentration range in the anode feed gas than reported in literature. The obtained results provide practical information for fuel cell engineers and fuel cell system designers since optimization of working conditions could assist to further minimize losses observed on the polycycles and fuel cell systems and thereby improve performance and efficiency.

2. Experimental methods

This study was undertaken in the HySA Systems state-of-the-art fuel cell laboratory and test facility equipped with commercial single cell/stack testing stations (FuelCon and Greenlight Innovation) and in-house constructed single fuel cell testing setups. The HySA Systems laboratories have the capability for testing HT- and LT-PEM single fuel cells with electrode area of 5, 25 and 100 cm² as well as HT- and LT-PEM fuel cell stacks up to 5 kW_{el} power. The experimental tests can be performed and I_eV/power curves can be generated at various operating temperatures (200-200 °C), back pressures (0-5 barg), reactant gases compositions (CO, CO₂, CH₄, N₂ for anode, O₂, N₂, air at the cathode), gas flow rates (0.005-100 SLPM for anode and 0.01-600 SLPM for cathode) and gas humidification levels (0-100% relative humidity). The results presented in this paper were obtained using a Greenlight Innovation G-400 fuel cell stack testing station with high temperature operation and integrated Cell Voltage Monitoring (CVM) capabilities. The station is equipped with two cooling/heating loops where the external loop is filled with a water-glycol mixture and a heat transfer fluid is circulated in the internal loop. Stack resistance at 1 kHz was measured using a Schuetz Messtechnik MR 2212 W AC milliohm meter.

The validation study was carried out on a 48-cell 1 kW electrical power HT-PEMFC stack made up of commercial BASF MEAs, Celtec[®]-P 2100 (96 cm²

electrode area; 905 mm thick). Based on technical specifications declared by the producer, the catalyst on the cathode side is made of a Pt-alloy with a loading of $0.75 \text{ mgPt cm}^{-2}$ whereas the anode Pt catalyst loading is 1.0 mgPt cm^{-2} . Currently the commercial BASF MEAs possess the highest performance (0.6 A cm^{-2} at 0.6 V and $160 \text{ }^\circ\text{C}$) and long-term stability (over 20 000 h with 6 mV h^{-1} voltage drop at $160 \text{ }^\circ\text{C}$) in comparison with products from other suppliers offering HT-MEAs in the market; for example FuMA-Tech GmbH (Fumea[®] MEA e 0.6 A cm^{-2} at 0.6 V and $160 \text{ }^\circ\text{C}$, durable for 900 h test at $160 \text{ }^\circ\text{C}$), Advent Technologies SA (TPS[®] MEA e 0.35 A cm^{-2} at 0.6 V and $180 \text{ }^\circ\text{C}$, over 4000 h with 9 mV h^{-1} voltage drop at $180 \text{ }^\circ\text{C}$) or Danish Power Systems[®] (Dapozol[®] MEA e 0.4 A cm^{-2} at 0.6 V and $160 \text{ }^\circ\text{C}$, >5000 h lifetime in continuous operation). This explains why BASF Celtec[®] MEAs are most often used for benchmarking new developments in the HT-PEMFC field and why most publications that concern HT-PEMFC technology involves the application of this commercially available product. Graphite bipolar plates with multi-channel meander flow field pattern were machined using a Schunk FU 4369 HT material to supply reactant gases to the stack electrodes. The flow pattern of the bipolar plate is shown in Fig. 1. Locally manufactured silver plated aluminium current collectors with 100 cm^2 surface area were used to integrate the fuel cell stack with the electronic load installed on the testing station. The MEAs, bipolar plates and current collectors were sandwiched between two aluminium end plates with the help of four threaded stainless steel rods and nuts; springs were used to apply suitable compression between stack components. Suitable stack compression of 6 N mm^{-2} is important in order to minimize contact resistance between the bipolar plates and the MEAs. The stack parameters are presented in Table 1. More detailed description of the design and construction of the validated, externally oil cooled stack based on a design from ZSW is available elsewhere [7,8]. The modelling assumptions and stack concept design were verified with experimental results. During this study specially designed bipolar plates were incorporated into the stack to monitor cell temperature distribution within the electrode active area.

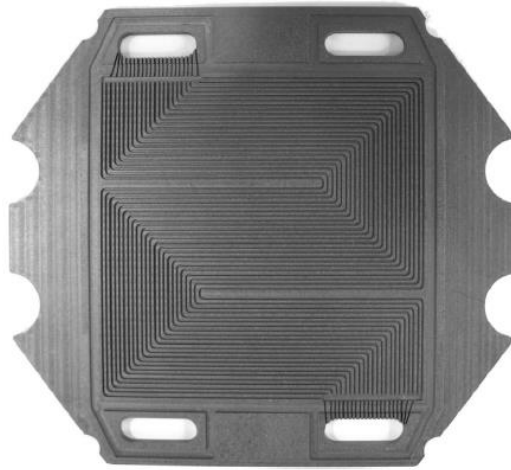


Fig. 1 – Bipolar plate flow field pattern based on the design from ZSW.

Table 1 – HT-PEMFC stack technical specification.	
HT-PEMFC stack	
Number of cells 48	
Active cell area 96 cm ²	
OCV 0.9 V	
Nominal cell voltage 0.6 V	
Minimum cell voltage 0.45 V	
Nominal current 40 A continuous (maximum 65 A short time)	
Nominal power 1 kW (~20 W/cell at $U_{\text{cell}} = 0.50\text{--}0.55$ V)	
Operation temperature 90–160 °C	
Cooling externally oil cooled, maximum 5 K difference between inlet and outlet	
Dimension 20 cm × 19 cm × 15 cm	
Weight 6.5 kg	
Stack compression pressure 6 N mm ⁻²	
Anode gas supply:	Cathode gas supply:
Dry hydrogen or reformat	Dry air
Minimum flow rate calculated for 0.2 A cm ⁻²	Minimum flow rate calculated for 0.2 A cm ⁻²
Maximum flow rate 50 SLPM	Maximum flow rate 200 SLPM
Utilization: 40–90%	Utilization: 25–60%
Pressure ambient up to 0.5 bar _g	Pressure ambient up to 0.6 bar _g

A temperature deviation smaller than 10 K was obtained experimentally at a specific heat production of 0.248 W cm⁻² and a linear extrapolation was made to predict temperature deviation would be less than 15 K at a specific heat production of 0.4 W cm⁻² [7,8]. The currently investigated stack was assembled without the bipolar plates that enabled cell temperature distribution monitoring.

To activate the MEA and ensure stable cell behaviour and reproducibility of results, after installation on the testing station, a galvanostatic high temperature break-in/conditioning procedure was applied. During the break-in, the performance of MEA increases but the nature of the process is not known yet. The humidification of the membrane by the produced water, removal of impurities from the catalyst,

ripening of the catalyst and redistribution of the electrolyte are possible reasons for the increased performance of the MEA [17,18]. The stack was heated up to 120 °C at a rate of about 5 K min⁻¹ in a nitrogen atmosphere. Once the stack reached 120 °C, pure hydrogen and air preheated to 100 °C was supplied to the anode and cathode, respectively at stoichiometries of 1.25 and 2.0 and ambient pressure. Further temperature increase to 140 °C was allowed and the stack was then operated for 10 h at a constant current density of 0.2 A cm⁻². After the described break-in procedure, measurements were performed.

It is now well-known that the formation of liquid water inside the stack can cause leaching out of the phosphoric acid from the PBI membrane which leads to irreversible degradation of the proton conductive properties of the membrane, and in turn influences the lifetime of the stack [3,4]. Although water is produced at the cathode during stack operation, excess water accumulation in the stack, due to condensation during 'start-up/shut down' procedures should be minimized to improve stack lifetime. To avoid conditions which induce the condensation of water during 'start-up and shut down', a systematic procedure was followed as proposed by Scholta et al. [19]. The procedure to generate polarization curves is described below. The HT-PEMFC stack was preheated to 100 °C in nitrogen atmosphere before each polarization curve was recorded. Dry gas was supplied to the anode and cathode at 100 °C. The stack temperature was increased by circulating Paratherm NF[®] heat transfer fluid through an external heating/cooling system. Once the minimum operation temperature of 100 °C was reached, the stack anode and cathode were supplied with the reactant gases. Dry hydrogen and air pre-heated to 100 °C were supplied to the anode and cathode, respectively at the minimum flow rate calculated for a current density of 0.2 A cm⁻² and ambient pressure, except measurements at elevated back-pressure values. The stack current was increased in 5 A steps to the nominal value of 40 A at which the required stack operational temperature could be controlled. While increasing the stack current, the single cell voltage was monitored in order to avoid a drop in the cell voltage below 0.5 V. The polarization curves were measured in galvanostatic load mode. Five minutes of stabilization time was used for every current value after a constant operation temperature was reached.

At OCV conditions the stabilization time was limited to 30 s to avoid electrode degradation. Minimum stoichiometries for anode and cathode were determined to be 1.25 and 2.00 and all measurements were performed at these stoichiometries for anode and cathode, respectively. When the stack was characterized at different CO concentrations, the suitable gas mixture was supplied to the anodes once the stack reached its required operation temperature at set current values.

In this work, the stack experimental results were used to validate a model developed by Rabiou et al. and general summary of the model as well as details of the model development can be found elsewhere [20]. The model is a 'zero-dimensional' model that focuses on the reaction kinetics in the MEA. This approach was selected due to its simplicity for the implementation of the Engineering Equation Solver (EES) modelling platform. The model framework is based upon the isothermal model developed by Mamlouk and Scott [21]. In the model, the hydrogen oxidation and oxygen reduction reaction kinetics are expressed using the Butler-Volmer equation, which allows for analysis of cell performance for different electrochemical surface areas and catalyst loadings. The approach of Cheddie and Munroe [22] which uses the solubility of various species in phosphoric acid is used to predict the membrane conductivity activity. The model is developed to calculate the cell voltage when operating at different conditions.

3. Results and discussion

As mentioned above, this paper focuses on the investigation of the effects and influence of various operating conditions on the HT-PEMFC stack performance, in particular on the CO tolerance and thereby its suitability to operate with reformat containing high concentrations of CO; in turn simplifying the reformat purification system and giving a significant advantage to HT-PEMFC stacks as compared to LT-PEMFCs. In the following sections, several experimental results are presented and discussed.

3.1. Effect of the anode and cathode stoichiometries on stack single cell voltage

The objective of this test was to determine the minimum stoichiometry values for electrode gas supplies which did not affect cell performance and thus allowed operation at the highest stack efficiency. The utilization curves of the stack were measured for the anode and cathode separately at 0.30 A cm^{-2} and stack temperature close to $160 \text{ }^{\circ}\text{C}$. The exact temperature value was not crucial in this test. It was however important to maintain the stack operating temperature close to the nominal value and to keep it stable during the experiment. For the cathode utilization curve measurement, the anode utilization was kept constant at 80%. In the case of the anode utilization curve measurement, the cathode utilization level was kept constant at 50%. The single cell maximum, mean and minimum voltages were monitored and recorded during all measurements. The measured values are presented in Fig. 2(a) and (b), for anode and cathode, respectively. The figures also show the stack and cathode exhaust gas temperature values.

The results obtained for anode utilization curve show that there is no influence of anode stoichiometry on the single cell voltage for stoichiometries ranging from 1.25 to 2.5. For stoichiometries lower than 1.25, a cell voltage drop of 27 mV was observed. The decrease of anode stoichiometry to the value close to 1.0 did not cause any significant drop of maximum or mean cell voltage. The minimum cell

voltage indicates the possibility of hydrogen starvation in the stack. This condition can be very harmful to the stack and may lead to oxygen evolution at the anode side which irreversibly damages the catalyst and catalyst support [23]. Based on these tests, the minimum anode stoichiometry which did not cause decrease of the stack performance was found to be 1.25. During the experiments, a stable stack temperature (ca. 160 °C) and cathode exhaust gas temperature (ca. 140 °C) was noted.

In the case of the cathode side, the results obtained for cathode utilization curve revealed that cathode stoichiometry does not affect single cell voltage for stoichiometries ranging from 2.0 to 4.0. For stoichiometries lower than 2.0, a minimum cell voltage drop of 59 mV was observed. Here, it can be assumed that the effect for higher current densities would be considerably more significant. The effect of the cell voltage drop at low cathode stoichiometries may be due to slower thermodynamics and kinetics of the fuel cell reactions as well as slower gas diffusion processes [23]. The influence of cathode stoichiometry on maximum and mean cell voltage for stoichiometry values below 2.0 was negligible. During the experiments, it was also observed that the stack temperature increased from 140 °C to 160 °C, with decreasing cathode stoichiometry. At the same time, the cathode exhaust temperature decreased from 147 °C to 140 °C due to quite a significant change of air flow rate from 39 to 95 SLPM. Nevertheless, it was possible to observe the effect of cathode stoichiometry on stack performance and to determine the minimum cathode stoichiometry at which the stack could operate without performance loss, which was found to be 2.0 for our conditions.

3.2. Temperature effect on stack performance

Temperature is a key parameter that influences the HT-PEMFC performance. Higher temperature improves electrode kinetic performance and increases the ionic conductivity of the membrane and electrodes. Increased temperature also results in exponentially higher exchange current density (I_0) and improves mass transport properties [24,25].

The stack polarization curves were measured at different operating temperatures. The results of recorded stack voltage and stack power were plotted versus stack current, while the mean cell voltage and power density were plotted versus stack current density and are shown in Fig. 3(a) and (b), respectively. The stack power of 1 kW was measured at temperature 140 and 160 °C, Fig. 3(a). Measurements performed at 120 °C were limited to 30 A because of problems with temperature control at relatively low temperature and high current. A positive effect of temperature on stack performance can be easily observed. The higher the operating temperature was, the better the stack performance, although the difference was not significant. For example at a current density of 0.3 A cm⁻², the measured mean cell

voltages were 0.532, 0.542 and 0.569 V for 120, 140 and 160 °C, respectively. This increase in temperature (DT 1/4 40 °C) leads to an enhancement in power density of 5 mW cm⁻². The best stack performance was recorded at 160 °C and the measured power density at 0.4 A cm⁻² was 225 mW cm⁻². The temperature effect observed can be explained by the reduced charge transfer and proton transfer resistances [26].

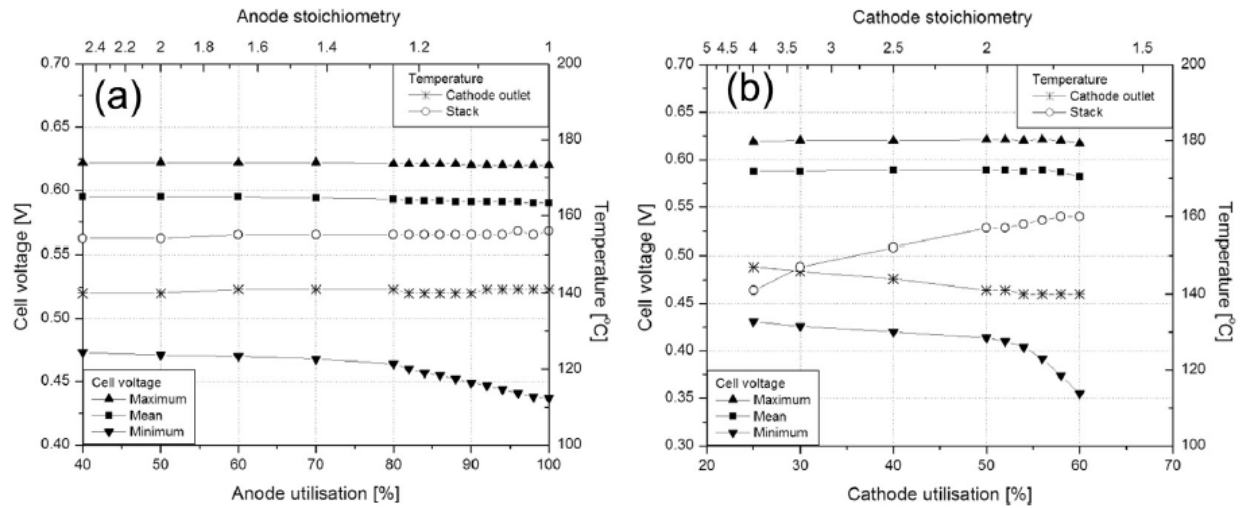


Fig. 2 – Stack cell voltages at different anode (a) and cathode (b) stoichiometries.

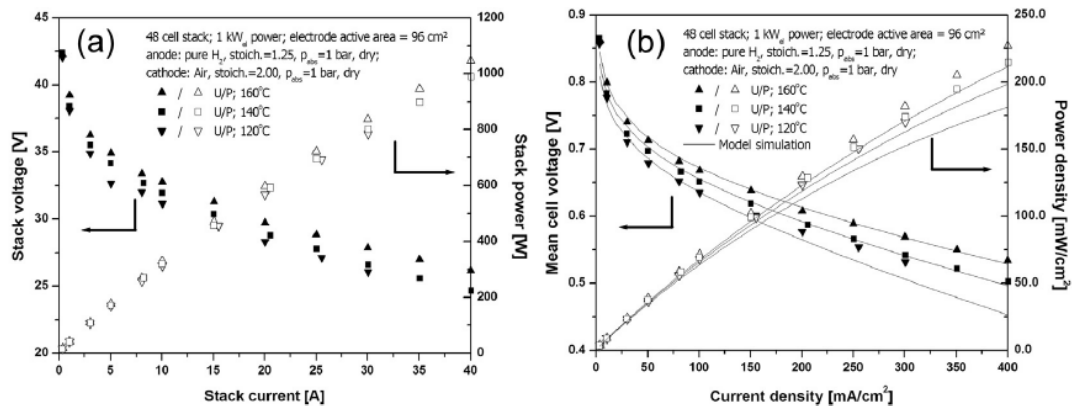


Fig. 3 – Stack (a) and single cell (b) polycurves measured at various operating temperatures from 120 to 160 °C.

The experimental results were compared to simulation results and as can be seen in Fig. 3; there is good agreement between the two. For 140 °C and 160 °C the model correctly predicts the stack voltage performance for the entire voltage range. This is not the same for lower temperatures (120 °C), where the performance is under predicted at high current densities. For 120 °C the model deviates from experimental results at about 150 mA cm⁻² where it starts to under predict the stack performance. This could be a result of increased temperature caused by

increasing the current density, which cannot be captured by the isothermal model. During testing the stack ohmic resistance, which is related to electrical resistance, contact resistance and the membrane proton conductivity, was measured at 1 kHz constant frequency with the aid of a MR 2212 W AC milliohm meter. This method is often used to determine cell resistance (R_{cell}) [27] although more detailed information about phenomena taking place inside the cell during stack operation could be obtained by measurement of the cell/stack impedance spectra at a wide frequency range [28]. The results are presented in Fig. 4. As illustrated in Fig. 4, the cell ohmic resistance drops with increasing stack operating temperature. Reduction of the cell resistance from ca. $0.19 \text{ } \Omega \text{ cm}^2$ measured at $120 \text{ } ^\circ\text{C}$ to $0.14 \text{ } \Omega \text{ cm}^2$ measured at $160 \text{ } ^\circ\text{C}$ was observed within the high current density region. Higher ohmic resistance for current density lower than 0.1 A cm^{-2} was measured for all temperatures. The decrease in resistance with increasing current density can be due to the increase of membrane conductivity when more water is produced at the cathode, as the current density increases [29]. The obtained results are in very good agreement with data presented by Oono et al. [26].

The temperature effect can also be observed for individual cell voltages of the stack. It was observed that the cells at the extreme end of the stack had lower performance and the cell voltages were always lower than the mean cell voltages of the stack. Fig. 5 shows results of the cell voltage measurement at 0.4 A cm^{-2} and $160 \text{ } ^\circ\text{C}$ stack temperature. As it can be seen, the cell voltage at the extreme cells is 35 mV lower than the mean cell voltage measured for the stack. The measurement of the cell temperatures revealed that the stack has a temperature profile, which indicates the temperature is not even along the stack. Lower stack temperatures were recorded for extreme cells.

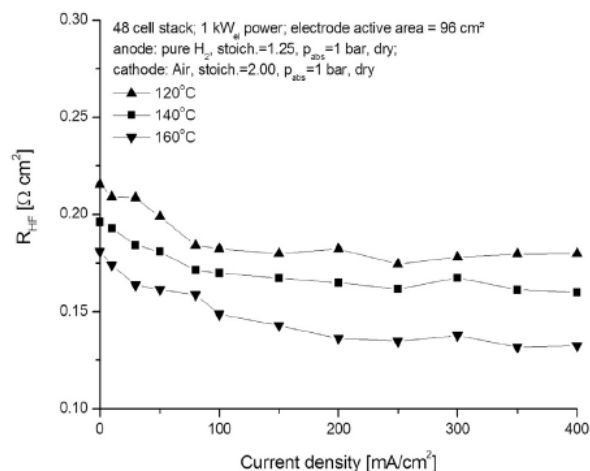


Fig. 4 – Cell high frequency resistances as a function of current density measured at three different temperatures.

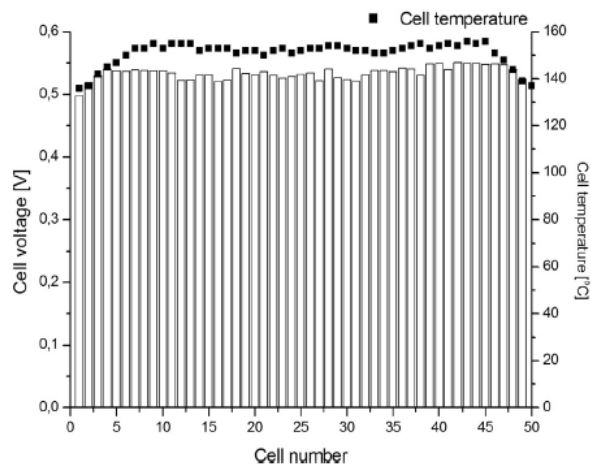


Fig. 5 – Individual cell voltages and stack temperature profile recorded at 0.4 A cm^{-2} current density and $160 \text{ } ^\circ\text{C}$ stack temperature.

The reason for this may be due to increased convection on both sides as well as the location of media (gases, cooling oil) connections. This information should be used to improve the stack design in the future and ensure even temperature for all cells within the stack.

3.3. Influence of reactant gas pressure on stack performance

Pressure is another factor that significantly influences the performance of the PEMFC. The pressure of reactants supplied to stack electrodes influences the cell potential according to the Nernst equation:

$$E = E_0 + \frac{RT}{nF} \ln \left(\frac{P_{H_2} P_{O_2}^{0.5}}{P_{H_2O}} \right)$$

where: E_0 is the open circuit voltage (V), R is the universal gas constant ($8.3145 \text{ J mol}^{-1} \text{ K}^{-1}$), T is the fuel cell temperature (K), n is the number of electrons taking part in the reaction, F is the Faradic constant (96485 C mol^{-1}) and P is the partial pressure of reactants and product species (bar). Moreover elevated pressure causes increase of reactant gas concentration on electrodes, thereby improving mass transport of gaseous species resulting in an increase in the exchange current density as well as improving electrode reaction kinetics [30].

Fig. 6(a) and (b) shows the effect of three different operating pressure values on the stack performance. Operation at elevated pressures up to 0.5 barg increased the stack voltage by 6% in comparison with operation at ambient pressure. The best stack performance was recorded at $160 \text{ }^\circ\text{C}$ and 0.5 barg pressure; a power density of 250 mW cm^{-2} was measured at 0.4 A cm^{-2} . The effect of pressure on the stack operation can also be seen from the simulation results. Similar to the experimental results, increased pressure results to better stack performance. Even though the trend of the experimental and simulation results is the same, the model used for simulation over-predicted the stack cell voltage.

3.4. Stack performance at several CO concentrations

Tolerance to CO concentrations (up to 3%) is one of the many advantages of using HT-PEMFCs. At high operating temperatures, the thermodynamics of CO adsorption on the Pt anode catalyst is less favoured and the resistance to CO poisoning is higher than in conventional LT-PEMFC [31,32]. However these studies are either theoretical or performed on a single cell setup. To the best of the authors' knowledge, there is no detailed report on the CO tolerance of HT-PEMFC stacks, which is

absolutely necessary to demonstrate its advantage and practicality especially for stationary applications.

A high temperature stack was evaluated against CO poisoning at various CO levels. The subsequent measured stack and cell polarization curves, at a stack operating temperature of 140 °C, with pure hydrogen and CO spiked hydrogen of various CO concentrations (0.1, 0.3, 0.5 and 1.0%) are shown in Fig. 7(a) and (b). A stable stack operation was observed for CO concentration reaching 1.0%, although a loss of performance of about 4% was already observed for a CO concentration of 0.1% at maximum stack power. It can be observed that at a current density of 0.2 A cm⁻² performance losses of 2.2, 6.0 and 8.4% were found for CO concentrations of 0.1, 0.3, 0.5%, respectively. Generating the performance curve for 1.0% CO concentration was not possible because the cell voltage dropped below the safe limit for the operation of the stack.

The predicted influence of carbon monoxide present in the anode gas feed is also shown in Fig. 7(b). Similar to the experimental results, presence of CO in the anode feed leads to a large decrease in stack performance. The decrease in performance is a result of active catalyst sites being covered by CO, even for small (0.1%) amounts of CO. As can be seen in Fig. 7, good agreement between the experimental and simulation results is obtained at low current densities for both the stack cell average voltage and power density. The model, however, fails to accurately predict the stack performance for high current density and for high CO concentration (1.0%) in the anode feed.

Fig. 8 represents the cell voltage loss versus current density at 140 °C for several CO concentrations, the data derived from Fig. 7. A similar figure was generated for higher operating temperature e 160 °C at similar CO levels in the anode feed gas (Fig. 9). It can be seen that the values of the cell voltage loss at lower temperatures are much higher than those obtained at 160 °C, as expected. For example at a current density of 0.15 A cm⁻² at 140 °C the cell voltage loss values were found to be 15, 34, 46, 84 mV whereas at 160 equal to 8, 29, 35, 41 mV at similar CO concentration.

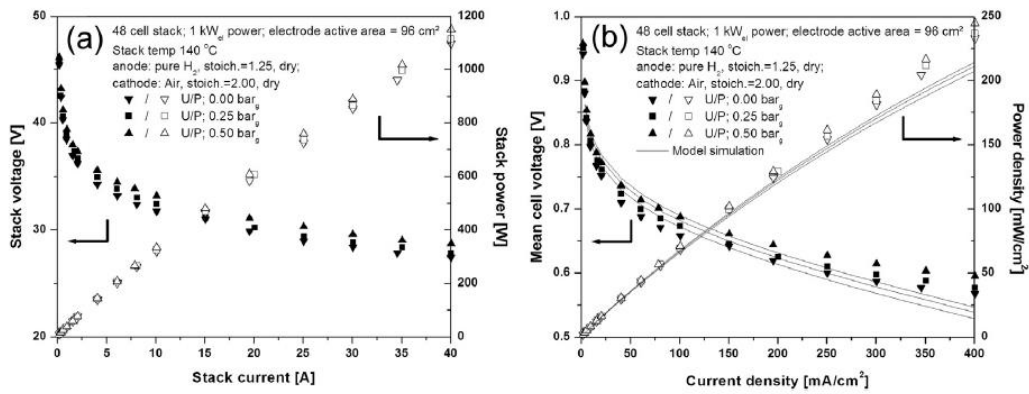


Fig. 6 – Stack (a) and single cell (b) polycurves measured at various operating pressures from 0 to 0.5 bar_g and 140 °C stack temperature.

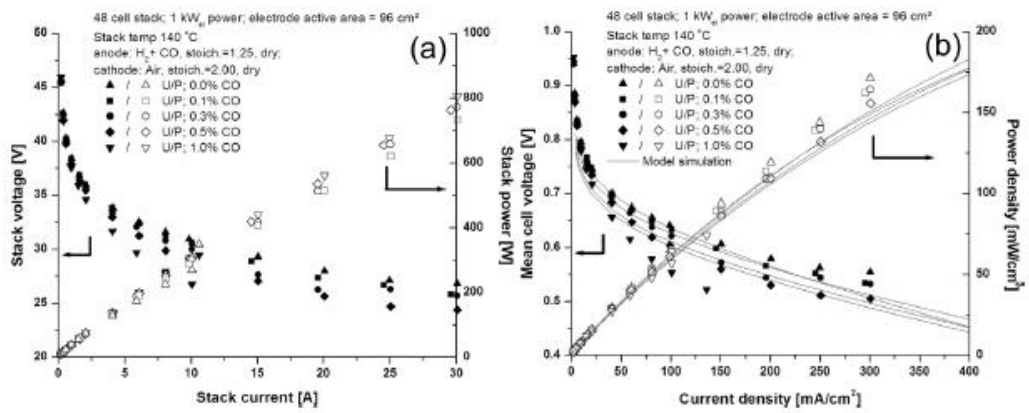


Fig. 7 – Stack (a) and single cell (b) polycurves at various CO concentrations from 0 to 1% in anode reactant gas measured at 140 °C stack temperature.

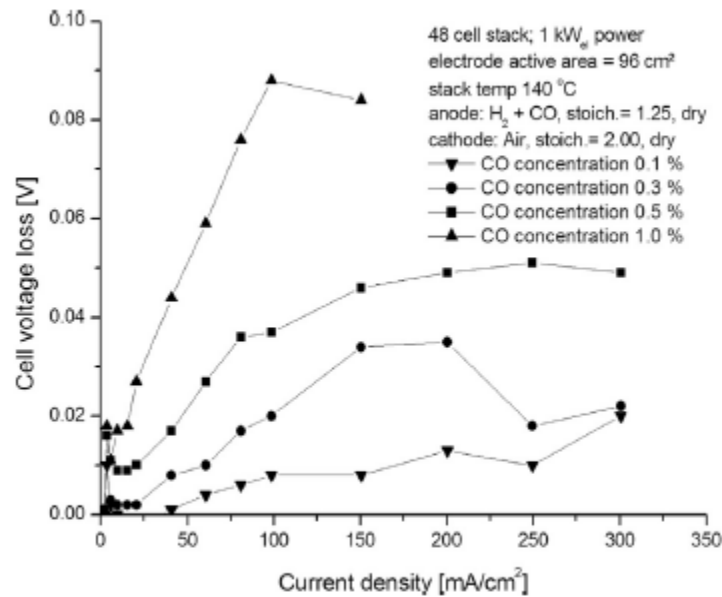


Fig. 8 – Cell voltage loss versus current density for different CO concentrations at 140 °C stack temperature.

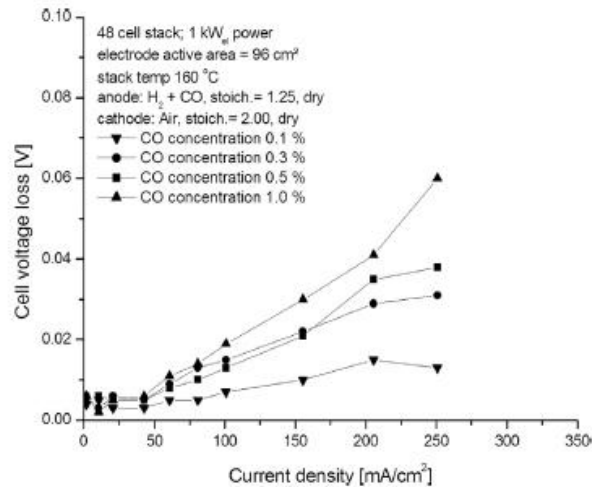


Fig. 9 – Cell voltage loss versus current density for different CO concentrations at 160 °C stack temperature.

This finding clearly indicates that higher operating temperature enhances the fuel cell performance and tolerance to CO while operating with higher CO concentration in the anode feed gas. The stack shows good CO tolerances of up to 0.5% at an operating temperature of 160 °C. This value of 0.5% CO tolerance is much lower than of the value of up to 3% CO reported by Li et al. [13] in single cell measurements and operating at 180 °C. Due to the limitations with operating the stack at temperatures above 160 °C, no experiments were performed at 180 °C, but are planned and will be reported later. The long-term stability tests and the study of the degradation mechanisms on 1 kW HT-PEMFC stack at different CO concentrations are ongoing at HySA Systems and results will be prepared for publication as soon as testing is completed.

4. Conclusions

In this work, an externally oil cooled 48 cell HT-PEMFC stack was validated for its performance and suitability of its integration with a reformer. The experiments were carried out at various anode (1e2.5) and cathode (1.6e4) stoichiometries; stack operating temperatures (120e160 °C); elevated gas pressures (0e0.5 barg) and CO concentrations (0e1.0%) in the anode feed gas. Polarization and power curves were measured and the parameters influencing the stack performance were analysed. The minimum stoichiometries for anode and cathode were experimentally determined to be 1.25 and 2.0. For these values the gas flow rate was found to be sufficient to avoid hydrogen or/and oxygen starvation conditions for the anode and cathode, respectively.

As expected, the stack temperature showed significant effects on the stack performance. The best stack performance was obtained at a power density of 225 mW cm⁻², at 160 °C and at 0.4 A cm⁻². The cell ohmic resistance measured at 1

kHz dropped with increased stack operating temperature and with increased current density up to 0.1 A cm^{-2} . For all temperatures at current densities higher than 0.1 A cm^{-2} the values of cell resistance were stable. As explained, this was thought to be due to a constant water-content level within the cell being reached and membrane conductivity remaining unchanged. It was found that the temperature of all the cells within the stack should be even as temperature variations affect the overall cell performance.

The effect of reactants pressure on stack performance was also investigated. Operations at elevated pressures increased the partial pressure of gases thus improving the thermodynamics and the kinetics of fuel cell reactions as well as the gas diffusion processes. The best stack performance was recorded at a power density of 250 mW cm^{-2} at $160 \text{ }^\circ\text{C}$, 0.5 barg , and 0.4 A cm^{-2} .

Stack tolerance to CO of various concentrations was studied and polarisation/power curves at different CO concentrations in the anode feed gas were measured. The stack operated stable at CO concentration reaching 1% although a loss of performance of about 4% was observed for low CO concentrations. Values of cell voltage loss at $140 \text{ }^\circ\text{C}$ were much higher than that obtained for $160 \text{ }^\circ\text{C}$, indicating that higher operating temperatures enhance fuel cell performance and tolerance to CO. The stack showed a reasonable CO tolerance of up to 0.5% CO at $160 \text{ }^\circ\text{C}$.

Acknowledgements

This work is supported by Hydrogen and Fuel Cell Technologies RDI Programme (HySA), funded by the Department of Science and Technology in South Africa (Project KP1-S03).

References

- [1] Oono Y, Sounaib A, Hori M. Influence of the phosphoric acid-doping level in a polybenzimidazole membrane on the cell performance of high-temperature proton exchange membrane fuel cells. *Journal of Power Sources* 2009;189:943e9.
- [2] He R, Li Q, Xiao G, Bjerrum NJ. Proton conductivity of phosphoric acid doped polybenzimidazole and its composites with inorganic proton conductors. *Journal of Membrane Science* 2003;226:169e84.
- [3] Galbiati S, Baricci A, Casalegno A, Marchesi R. Experimental study of water transport in a polybenzimidazole-based high temperature PEMFC. *International Journal of Hydrogen Energy* 2012;37:2462e9.
- [4] Chen CY, Lai WH. Effects of temperature and humidity on the cell performance and resistance of a phosphoric acid doped polybenzimidazole fuel cell. *International Journal of Hydrogen Energy* 2010;195:7152e9.
- [5] Supra J, Janßen H, Lehnert W, Stolten D. Temperature distribution in a liquid-cooled HT-PEFC stack. *International Journal of Hydrogen Energy* 2013;38:1943e51.
- [6] Andreasen SJ. Design and control of high temperature PEM fuel cell system. Ph.D thesis. Aalborg University, ISBN 87- 89179-78-1; 2009.
- [7] Scholta J, Messerschmidt M, Jorissen L, Hartnig Ch. Externally cooled high temperature polymer electrolyte membrane fuel cell stack. *Journal of Power Sources* 2009;190:83e5.
- [8] Pasupathi S, Bujlo P, Ulleberg O, Scholta J. Validation of a HT-PEMFC stack for CHP applications. In: 18th World hydrogen energy conference 2010. DOI: 1866-1793. ISBN: 978-3-89336-651-4.
- [9] Scholta J, Zhang W, Jorissen L, Lehnert W. Conceptual design for an externally cooled HT-PEMFC stack. *ECS Transactions* 2008;12:113e8.
- [10] Rossetti I, Biffi C, Tantardini GF, Raimondi M, Vitto E, Alberti D. 5 kWe p 5 kWt reformer-PEMFC energy generator from bioethanol first data on the fuel processor from a demonstrative project. *International Journal of Hydrogen Energy* 2012;37:8499e504.
- [11] Karstedta J, Ogrzewalla J, Severina C, Pischinger S. Development and design of experiments optimization of a high temperature proton exchange membrane fuel cell auxiliary power unit with onboard fuel processor. *Journal of Power Sources* 2011;196:9998e10009.
- [12] Yim SD, Sohn YJ, Yoon YG, Um S, Kim CS, Lee WY. Operating characteristics of 40 W-class PEMFC stacks using reformed gas under low humidifying conditions. *Journal of Power Sources* 2008;178:711e5.
- [13] Li Q, He R, Gao JA, Jensen JO, Bjerrum NJ. The CO poisoning effect in PEMFCs operational at temperatures up to 200 ° C. *Journal of the Electrochemical Society* 2003;150(12):A1599e605.

- [14] Andreasen SJ, Vang JR, Kær SK. High temperature PEM fuel cell performance characterization with CO and CO₂ using electrochemical impedance spectroscopy. *International Journal of Hydrogen Energy* 2011;36:9815e30.
- [15] Mocoteguy P, Ludwig B, Scholta J, Barrera R, Ginocchio S. Long term testing in continuous mode of HT-PEMFC based H₃PO₄/PBI Celtec-P MEAs for CHP applications. *Fuel Cells* 2009;09:325e48.
- [16] Mocoteguy P, Ludwig B, Scholta J, Nedellec Y, Jones DJ, Roziere J. Long term testing in dynamic mode of HT-PEMFC based H₃PO₄/PBI Celtec-P MEAs for micro-CHP applications. *Fuel Cells* 2010;10:299e311.
- [17] Boaventura M, Mendes A. Activation procedures characterization of MEA based on phosphoric acid doped PBI membranes. *International Journal of Hydrogen Energy* 2010;35:11649e60.
- [18] Tingelo T, Ihonen JK. A rapid break-in procedure for PBI fuel cells. *International Journal of Hydrogen Energy* 2009;34:6452e6.
- [19] Scholta J, Kuhn R, Wazlawik S, Jö rissen L. Startup-procedures for a HT-PEMFC stack. *ECS Transactions* 2009;17:325e33.
- [20] Myalelo MV, Nkosikho D, Ikhu-Omoregbe D, Rabiou A. Optimization studies on the performance of a high temperature proton exchange membrane fuel cell. In: *International science and technology conference*. ISSN2146-7382 2011. p. 608e13.
- [21] Sousa T, Mamlouk M, Scott K. A dynamic non-isothermal model of a laboratory intermediate temperature fuel cell using PBI doped phosphoric acid membranes. *International Journal of Hydrogen Energy* 2010;35:12065e80.
- [22] Cheddie DF, Munroe NDH. A two-phase model of an intermediate temperature PEM fuel cell. *International Journal of Hydrogen Energy* 2007;32:832e41.
- [23] Zhang J, Xie Z, Zhang J, Tang Y, Song C, Navessin T, et al. High temperature PEM fuel cells. *Journal of Power Sources* 2006;160:872e91.
- [24] Lobato J, Canizares P, Rodrigo MA, Linares JJ. PBI-based polymer electrolyte membranes fuel cells. Temperature effects on cell performance and catalyst stability. *Electrochimica Acta* 2007;52:3910e20.
- [25] Su A, Ferng YM, Hou J, Yu TL. Experimental and numerical investigations of the effects of PBI loading and operating temperature on a high-temperature PEMFC. *International Journal of Hydrogen Energy* 2012;37:7710e8.
- [26] Oono Y, Fukudaa T, Sounaib A, Hori M. Influence of operating temperature on cell performance and endurance of high temperature proton exchange membrane fuel cells. *Journal of Power Sources* 2010;195:1007e14.
- [27] Lobato J, Canizares P, Rodrigo MA, Linares JJ, Manjavacas G. Synthesis and characterization of poly[2,2-(m-phenylene)-5,5-bibenzimidazole] as polymer

electrolyte membrane for high temperature PEMFCs. *Journal of Membrane Science* 2006;280:351e62.

[28] Kondratenko MS, Gallyamov MO, Khokhlov AR. Performance of high temperature fuel cells with different types of PBI membranes as analyzed by impedance spectroscopy. *International Journal of Hydrogen Energy* 2012;37:2596e602.

[29] Chen CY, Lai WH. Effects of temperature and humidity on the cell performance and resistance of a phosphoric acid doped polybenzimidazole fuel cell. *Journal of Power Sources* 2010;195:7152e9.

[30] Taccani R, Zuliani N. Effect of flow field design on performances of high temperature PEM fuel cells: experimental analysis. *International Journal of Hydrogen Energy* 2011;36:10282e7.

[31] Dhar HP, Christner LG, Kush AK, Maru HC. Performance study of a fuel cell Pt on C anode in presence of CO and CO₂, and calculation of adsorption parameters for CO poisoning. *Journal of the Electrochemical Society* 1986;133:1574e82.

[32] Bellows RJ, Marucchi-Soos EP, Terence BD. Analysis of reaction kinetics for carbon monoxide and carbon dioxide on polycrystalline platinum relative to fuel cell operation. *Journal of Industrial and Engineering Chemistry Research* 1996;35:1235e42.